31st Annual International Conference of the IEEE EMBS
Minneapolis, Minnesota, USA, September 2-6, 2009

Refining Enamel Thickness Measurements from B-Mode Ultrasound Images

Jeremy Hua, Ssu-Kuang Chen, and Yongmin Kim, *Fellow, IEEE*

Abstract—Dental erosion has been growing increasingly prevalent with the rise in consumption of heavy starches, sugars, coffee, and acidic beverages. In addition, various disorders, such as Gastroenterological Reflux Disease (GERD), have symptoms of rapid rates of tooth erosion. The measurement of enamel thickness would be important for dentists to assess the progression of enamel loss from all forms of erosion, attrition, and abrasion. Characterizing enamel loss is currently done with various subjective indexes that can be interpreted in different ways by different dentists. Ultrasound has been utilized since the 1960's to determine internal tooth structure, but with mixed results. Via image processing and enhancement, we were able to refine B-mode dental ultrasound images for more accurate enamel thickness measurements. The mean difference between the measured thickness of the occlusal enamel from ultrasound images and corresponding gold standard CT images improved from 0.55 mm to 0.32 mm with image processing (p = 0.033). The difference also improved from 0.62 to 0.53 mm at the buccal/lingual enamel surfaces, but not significantly (p = 0.38).

Keywords- B-mode ultrasound, enamel, dental ultrasound, image analysis

I. INTRODUCTION

Ultrasound has shown potential for being able to diagnose and monitor external, as well as internal, damage to teeth, including decalcification, abrasions, fractures, and caries [1,2]. A particular use is examining the enamel layer of the tooth to detect signs of enamel erosion or abrasion caused by various factors over time. Occurrence of enamel erosion originates from intrinsic sources such as stomach acid from vomiting or Gastroesophageal Reflux Disease (GERD). Patients who complained of having symptoms of GERD were found to have greater overall tooth wear and were more likely to have tooth wear involving dentin than those who did not suffer from GERD [3]. Enamel loss is a common symptom in acid reflux, and quantitatively evaluating enamel loss with ultrasound could help diagnose patients easily. Erosion due to external factors, e.g., acidic food and drinks and excessive brushing [4], is common occurrence as well. Sodas and fruit juices are heavily consumed these days, and the low pH of such beverages assist in the permanent decalcification of tooth enamel [5,6,7]. Current techniques for measuring enamel loss consist of dentists performing subjective observations with various indexing systems, including the Smith and Knight Index [8], and Eccles Index [9]. The many different indexes are summarized by Hooper *et al.* [10]. Often, they cannot be compared directly. However, the use of ultrasound imaging for enamel measurement has potential to become a standardized measure, which can be incorporated into a routine dental examination. The dental clinician can measure the progression of tooth substance loss over time to better understand and diagnose various erosion, abrasion and attrition-related problems.

Many researchers have attempted to use ultrasound as a non-ionizing imaging method to measure enamel thickness. Specific research targeted towards characterizing the internal structures of the tooth started as early as the 1960's with the use of ultrasound [11] and had mixed results. Various researchers determined that the probes used for pulse-mode dental ultrasound were difficult to position reproducibly, making enamel thickness measurements unreliable at small distances [12]. This dependency on transducer position turned some of the focus towards B-mode ultrasound with 1D array transducers to reduce the reliance on a single element transducer. Culjat *et al*. [1] performed a circumferential scan around a human tooth to produce a 2D representation of the enamel layer with good results. It would be useful to design an image processing/analysis algorithm to refine obtained ultrasound images for more accurate measurements. In this paper, we present such a technique that filters grayscale, B-mode ultrasound images of extracted human teeth to improve the accuracy of enamel thickness measurements *in vitro*.

II. METHODS

A. Computed Tomography Image Acquisition

X-ray Computed Tomography (CT) images were used as the gold standard for this study. CT is commonly used in oral and maxillofacial imaging and is effective for discerning the internal structures of teeth, although it is ionizing and not ideal for repeated exposure to patients. CT images of five extracted human teeth were obtained with the CB MercuRay system (Hitachi Medical Systems America, Twinsberg, Ohio). The voltage and tube current settings were set to 100 kV and 15 mA, respectively, with an

Manuscript received April 23, 2009. This work was supported in part by the Mary Gates Research Endowment, and by the National Institute of Health under Grant DK-070082.

J. Hua is with the Department of Bioengineering, University of Washington, Seattle, WA 98195 USA (e-mail: jhua27@ u.washington.edu).

S. K. Chen is with the Div. of Oral Radiology, Dept. of Oral Medicine, University of Washington, Seattle, WA 98195 USA (e-mail: cskchen@ u.washington.edu).

Y. Kim is with the Department of Bioengineering, University of Washington, Seattle, WA 98195 USA (e-mail: ykim@ u.washington.edu).

exposure time of 9.6 seconds. Two of the teeth were premolars, two were molars, and the fifth was a molar containing a metal amalgam insert that generated a lot of artifacts. The roots of the teeth were separately inserted and adhered to foam blocks. The blocks were aligned on the MercuRay platform parallel with the platform edge. DICOM image viewing was performed using UniSight DICOM viewer (EBM Technologies USA, Honolulu, Hawaii).

B. Phantom preparation

The foam blocks were lined up along the bottom of an acrylic container parallel to its edges and adhered in order to prevent movement. The container was filled with 4% Knox®-brand gelatin until the teeth were completely submerged. The entire system was then cooled overnight. The blocks acted as references to ensure that the acquired CT images and ultrasound images were registered correctly.

C. Ultrasound Image Acquisition

Ultrasound image were obtained with the Hi Vision 8500 (Hitachi Medical Systems America, Twinsburg, OH) using a EUP-L54M 13-MHz linear-array transducer. The transducer was secured in place with the transducer surface parallel to the ground and with the face nearly touching the gelatin surface of the acrylic container. Water was added to the container to improve the acoustic coupling between the transducer and the gelatin. The container was moved to a position such that the transducer was located at one end of the container. The container was then shifted at 1-mm intervals in the elevational direction of the transducer as images were acquired each time. The result was a set of cross-sectional ultrasound images that corresponded very well with the obtained CT images.

D. Image Processing

The primary goal with processing the raw ultrasound images is to refine the dentin-enamel junction (DEJ) for accurate enamel thickness measurement (Fig. 1) by sharpening the enamel boundary while maintaining the structural detail [13].

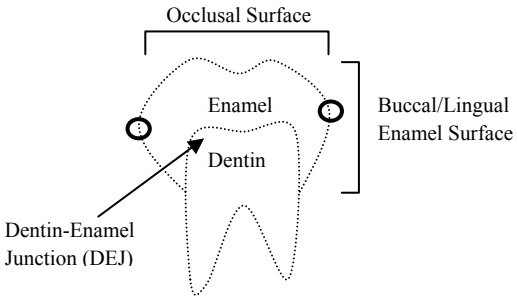

Figure 1. Basic anatomy of the tooth and relevant oral surfaces. Circles represent the left and rightmost points of the enamel surface.

The filter kernels used in this algorithm were 3x3 Laplacian (Fig. 2(a)) for omnidirectional edge detection, 3x3 Sobel vertical gradient for horizontal edge enhancement (Fig. 2(b)), and 5x5 boxcar for smoothing (Fig. 2(c)). The flow diagram of our image processing algorithm is shown in Figure 3. The first step was to apply the Laplacian kernel to the original ultrasound image (Fig. 4(a)), where Fig. 4(b) shows the result. The original image was then convolved with the Sobel vertical gradient kernel (Fig. 4(c)), which was smoothed with the 5x5 boxcar averaging kernel (Fig. 4(d)). The smoothed Sobel image was added to the Laplacian kernel output and multiplied by the original image after being scaled (Fig. 4(e)). Figure 4(f) is the corresponding CT image of the identical tooth cross section.

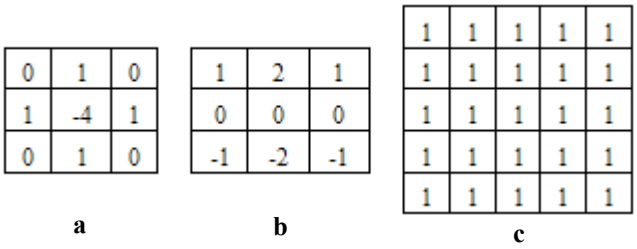

Figure 2. The filter kernels used in this study. (a) 3x3 Laplacian, (b) 3x3 Sobel vertical gradient, and (c) 5x5 boxcar.

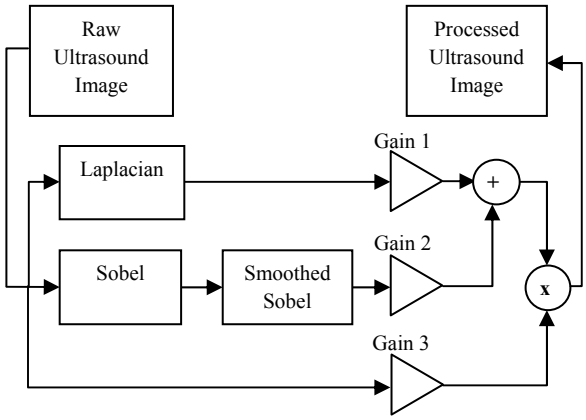

Figure 3. Flow diagram of image processing algorithm, with Gain 1 = 0.15, Gain 2 = 0.15, and Gain 3 = 0.07.

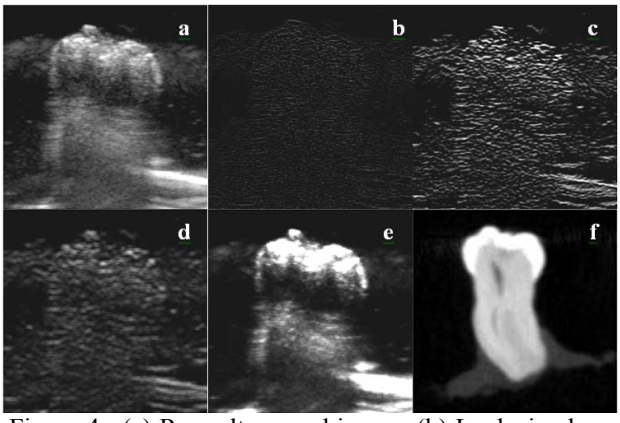

Figure 4. (a) Raw ultrasound image. (b) Laplacian kernel output of (a). (c) Sobel output of (a), and then, (d) smoothed with a 5x5 averaging kernel. (e) Sum of (b) and (d) multiplied by (a) after scaling. (f) CT image of the cross section corresponding to (a).

E. Enamel Thickness Measurement

Four dentists were asked to perform the enamel thickness measurements on ten image sets. Each set consisted of one raw ultrasound image, one processed ultrasound image, and one CT image of a single corresponding tooth cross section. The enamel measurement system consisted of using ImageJ [14] and SeedSuite [15]. A total of 30 images were provided to each observer in random order.

The images were marked prior to measurements by the observers to ensure that measurements were performed at pre-determined locations (Fig. 5(a)). For each image, the left and rightmost points (buccal and lingual portions of tooth) of the enamel layer were automatically located, thus creating two initial landmarks (Fig. 1). This was performed with Seedsuite, which provided feedback on the pixel coordinates of the two landmarks. A visible line was inserted connecting the two points (Line A), and a line (Line B) was inserted orthogonal to and at the midpoint of Line A. Line C was inserted parallel to Line A, intersecting Line B at a point 1 mm lower than Line A. The observer was asked to measure the enamel thickness along Line B using ImageJ, forming Length 1. The observer was then asked to measure the enamel thickness of the left and right sides of the enamel layer along Line C, creating Length 2a and 2b. This was repeated for each of the 30 images. An example image provided to the observer is shown in Figure 5(b).

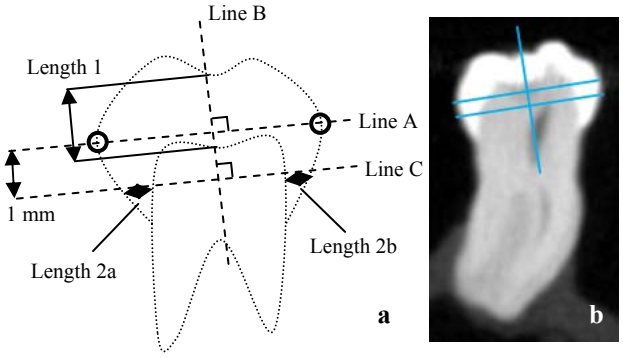

Figure 5. (a) Schematic of the markings added to the images before measurement by observers. The dotted lines represent the tooth similar to Fig. 1, and the three dashed lines are added directly to each image. Line A passes through the left and rightmost points of the enamel surface. Line B bisects Line A perpendicularly. Line C is located 1 mm below Line A. Length 1, 2a, and 2b designate measurements recorded by observers. (b) Example image provided to observer.

III. Results

A. Enamel Thickness Measurement

Each of the ten sets of images consisted of a raw ultrasound image, a processed ultrasound image, and a CT image of a selected tooth cross section. Each of these images had three total measurements: Length 1, 2a, and 2b, where Length 1 is of the occlusal enamel and Length 2a and 2b measurements are at either the buccal or lingual enamel surface. For each enamel thickness measurement from an ultrasound image, the difference in measured length was calculated in relation to the measured distance in the subsequent CT image. The mean of these values for each observer was averaged into two groups: those of the Length 1 measurements and those of the Length 2a or 2b measurements. The Length 2a and 2b measurements were combined because they are physically indistinguishable, as it was not known which side of the tooth was buccal and which was lingual.

The results are summarized in Table 1 for each of the observers. Measurements from the tooth containing the metal amalgam insert were excluded from data analysis. For the Length 1 measurements performed with raw ultrasound images, the difference in length from the gold standard CT images ranged from 0.39 to 0.67 mm, with a mean of 0.55 mm. The difference with the processed images ranged from 0.19 to 0.43 mm with a mean of 0.32 mm. For the Length 2a/2b measurements, the difference ranged from 0.50 to 0.87 mm (mean = 0.59 mm) with the raw ultrasound images, and from 0.46 to 0.61 mm (mean = 0.53 mm) with the processed ultrasound images. A two-tailed, unequal variance t-test between the raw and processed images of Length 1 showed $p = 0.033$, and for Length 2a/2b showed $p = 0.38$.

Table I DIFFERENCE FROM CT IMAGE (mm)

Observer No.	*Raw Ultrasound Images*		*Processed Ultrasound Images*	
	Length 1	**Length 2/3**	**Length 1**	**Length 2/3**
1	0.59	0.50	0.27	0.46
2	0.39	0.62	0.40	0.54
3	0.54	0.49	0.19	0.61
4	0.67	0.87	0.43	0.49
Mean	0.55	0.62	0.32	0.53

Some ultrasound images contained artifacts that were observed to disrupt the enamel boundary in the images. Figure 6 contains possible air bubbles near the enamel boundaries that were trapped in the gelatin medium, while these air bubbles are not present in the CT image.

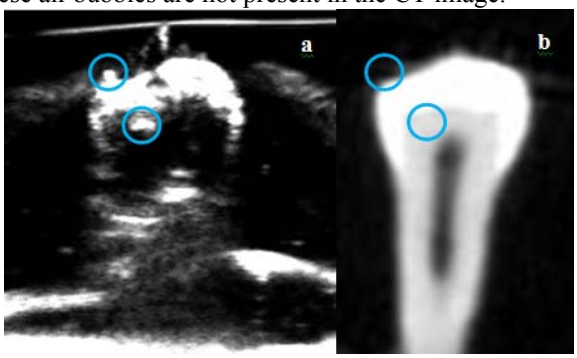

Figure 6. Comparison between a processed ultrasound image and the corresponding CT image. (a) Possible air bubbles trapped in the gelatin are noted in the ultrasound image, (b) which were absent in the CT image.

IV. DISCUSSION

The ability to measure enamel thickness along the entire enamel surface would provide the most information to dentists. In this study, enamel thickness measurements were obtained at three locations on the images (Fig. 5). These locations were reliably determined based on two initial landmarks.

Table I shows that the mean difference between measured enamel at Length 1 in the CT images and the raw ultrasound images is 0.55 mm compared to 0.32 mm in the processed ultrasound images. The p-value ($0.033<0.05$) illustrates that processing ultrasound images significantly improves the accuracy of enamel thickness measurements at occlusal surfaces. While the mean difference between measured enamel thickness at Length 2a/2b improved from 0.62 mm in the raw ultrasound images to 0.53 mm in the processed images, the p-value ($0.38>0.05$) shows that it is not a statistically significant improvement. So while image processing significantly improves the accuracy of measured enamel thickness at occlusal surfaces, the same significant improvement is not apparent at buccal/lingual surfaces.

A disadvantage of using B-mode ultrasound is its poor ability to discern the thickness of enamel along the side of the tooth, from either the buccal or lingual planes. This can be observed at Length 2a/2b for both the raw and processed ultrasound images compared to the high contrast in CT images. This is an inherent limitation with ultrasound as the DEJ and enamel-gelatin boundaries along these planes are nearly parallel to the axial ultrasound beam direction. Without relocating the transducer position or rotating the tooth, obtaining information from the buccal and lingual planes is difficult. This poses a challenge as the buccal and lingual enamel surfaces are generally thinner than the enamel at the occlusal surface. Dental erosion would be expected to erode through the enamel and into the underlying dentin layer quicker at these areas, making it an important concern for future research.

We have performed *in vitro* enamel measurement in a gelatin-based medium rather than a water-based medium in order to reduce the loss of acoustic energy at the outer tooth boundary. One limitation from using gelatin or agar for this experiment is the presence of bubbles. Even though the water was degassed before being used to make the gelatin mixture, bubbles were still observed in the solidified medium. Figure 6 illustrates this problem, where the possible presence of bubbles can be observed near the enamel surface. If these bubbles had been located near the regions of measurements, much higher variance would have resulted depending on the observers' view.

We have shown that B-mode ultrasound could be a useful method for measuring enamel thickness at occlusal surfaces. By image processing and enhancement, we can significantly improve the accuracy of the observed enamel thicknesses. Measurement of enamel thickness at buccal and lingual enamel surfaces remains to be improved.

REFERENCES

[1] M. Culjat, R. S. Singh, D. C. Yoon, and E. R. Brown, "Imaging of human tooth enamel using ultrasound," *IEEE Trans. on Med. Imag*., vol. 22, pp. 526-529, 2003.

[2] S. R. Ghorayeb, C. A. Bertoncini, and M. K. Hinders, "Ultrasonography in dentistry," *IEEE Trans. Ultrason., Ferroelect. Freq. Contr,* vol. 55, pp. 1256-1266, 2008.

[3] R. Moazzez, D. Bartlett, and A. Anggiansah, "Dental erosion, gastro-oesophageal reflux disease and saliva: how are they related?" *Journal of Dentistry*, vol. 32, pp. 489-494, 2004.

[4] A. Vieira A, E. Overweg, J. L. Ruben, and M. Huysmans, "Toothbrush abrasion, simulated tongue friction and attrition of eroded bovine enamel in vitro," *Journal of Dentistry*, vol. 34, pp. 336-342, 2006.

[5] A. Lussi, T. Jaeggi, and M. Shaffner, "Diet and dental erosion," *Nutrition and Oral Health*, vol. 18, pp. 780-781, 2002.

[6] S. Wongkhantee, V. Patanapiradej, C. Maneenut, and D. Tantbirojn, "Effect of acidic food and drinks on surface hardness of enamel, dentine, and tooth-coloured filling materials," *Journal of Dentistry*, vol. 34, pp. 214-220, 2006.

[7] J. F. Tahmassebi, M. S. Duggal, G. Malik-Kotru, and M. Curzon, "Soft Drinks and dental health: A review of the current literature," *Journal of Dentistry,* vol. 34, pp. 2-11, 2006.

[8] B. G. Smith and J. K. Knight, "An index for measuring the wear of teeth," *British Dental Journal,* vol. 256, pp. 435-438, 1984.

[9] J. D. Eccles, "Dental erosion of nonindustrial origin. A clinical survey and classification," *J Prosthet Dent*., vol. 42, pp. 649-653, 1979.

[10] S. M. Hooper, N. Meredith, and D. C. Jagger, "The development of a new index for measurement of incisal/occlusal tooth wear," *Journal of Oral Rehabilitation*, vol. 31, pp. 206-212, 2004.

[11] G. Baum, I. Greenwood, S. Slawski, and R. Smirnow, "Observation of internal structures of teeth by ultrasonography," *Science*, vol. 139, pp. 495–496, 1963.

[12] C. Louwerse, M. Kjaeldgaard, and M. Huysmans, "The reproducibility of ultrasonic enamel thickness measurements: an in vitro study," *Journal of Dentistry*, vol. 32, pp. 83-89, 2004.

[13] R. C. Gonzalez and R. E. Woods, Digital Image Processing. Upper Saddle River, NJ: Prentice-Hall, 2008.

[14] M. D. Abramoff, P. J. Magelhaes, and S. J. Ram, "Image processing with ImageJ," *Biophotonics International*, vol. 11(7), pp. 36-42, 2004.

[15] I. Tutar, L. Gong, S. Narayanan, S. D. Pathak, P.S. Cho, K. Wallner, and Y. Kim, "Seed-based transrectal ultrasound-fluoroscopy registration method for intraoperative dosimetry analysis of prostate brachytherapy," *Med. Phys.,* vol. 35, pp. 840-848, 2008.